Eur. Phys. J. C 22, 47–54 (2001)
Digital Object Identifier (DOI) 10.1007/s100520100790

THE EUROPEAN PHYSICAL JOURNAL C

A measurement of $K^{*\pm}$ production in the hyperon beam experiment at CERN

The WA89 Collaboration

M.I. Adamovich[8], Yu.A. Alexandrov[8,a], S.P. Baranov[8,a], D. Barberis[3], M. Beck[5], C. Bérat[4], W. Beusch[2], M. Boss[6], S. Brons[5,b], W. Brückner[5], M. Buénerd[4], Ch. Busch[6], Ch. Büscher[5], F. Charignon[4], J. Chauvin[4], E.A. Chudakov[6,c], U. Dersch[5], F. Dropmann[5], J. Engelfried[6,d], F. Faller[6,e], A. Fournier[4], S.G. Gerassimov[8,f], M. Godbersen[5], P. Grafström[2], Th. Haller[5], M. Heidrich[5], E. Hubbard[5], R.B. Hurst[3], K. Königsmann[5,g], I. Konorov[5,8,f], N. Keller[6], K. Martens[6,h], Ph. Martin[4], S. Masciocchi[5,i], R. Michaels[5,c], U. Müller[7], H. Neeb[5], D. Newbold[1], C. Newsom[j], S. Paul[5,f], J. Pochodzalla[5,k], I. Potashnikova[5], B. Povh[5], R. Ransome[l], Z. Ren[5], M. Rey-Campagnolle[4,m], G. Rosner[7], L. Rossi[3], H. Rudolph[7], C. Scheel [n], L. Schmitt[7,f], H.-W. Siebert[6], A. Simon[6,g], V. Smith[1,o], O. Thilmann[6], A. Trombini[5], E. Vesin[4], B. Volkemer[7], K. Vorwalter[5], Th. Walcher[7], G. Wälder[6], R. Werding[5], E. Wittmann[5], M.V. Zavertyaev[8,a]

[1] University of Bristol, Bristol, UK
[2] CERN, 1211 Genève 23, Switzerland
[3] Genoa Univ./INFN, Dipt. di Fisica, 16146 Genova, Italy
[4] Grenoble ISN, 38026 Grenoble, France
[5] Heidelberg Max-Planck-Institut für Kernphysik, Postfach 103980, 69029 Heidelberg, Germany
[6] Universität Heidelberg, Physikalisches Institut, 69120 Heidelberg Germany[p]
[7] Universität Mainz, Institut für Kernphysik, 55099 Mainz, Germany
[8] Moscow Lebedev Physics Inst., 117924, Moscow, Russia

Received: 6 August 2001 / Revised version: 3 September 2001 /
Published online: 5 October 2001 – © Springer-Verlag / Società Italiana di Fisica 2001

Abstract. We report on a measurement of the differential cross sections of inclusive $K^{\pm}_{890}$ production in Σ^-, π^- and neutron beams. A strong leading particle effect was observed for K^-_{890} production by Σ^-. The measured x_F–distributions are compared with calculations based on the Lund model (PYTHIA) and the quark-gluon string model.

1 Introduction

Although a long time has passed since the discovery of strange particles, the strange sector still remains a relatively poorly explored region in hadron physics. The interaction properties have been measured for only a few of particles, and the underlying mechanisms need further clarification. The production of strange quarks and their subsequent hadronization in hadron–hadron collisions constitute an important benchmark test for phenomenological models describing soft phenomena [1]–[3]. The data supplied by the recent WA89 experiment at CERN significantly reduce the lack of experimental information in this field [32–34].

[a] Supported by Deutsche Forschungsgemeinschaft, contract number DFG 436 RUS 113/465/0-2(R), and Russian Foundation for Basic Research under contract number RFFI 00-02-04018

[b] Now at TRIUMF, Vancouver, B.C., Canada V6T 2A3

[c] Now at Thomas Jefferson Lab, Newport News, VA 23606, USA

[d] Now at Instituto de Fisica, Universidad Autonoma de San Luis Potosi, S.L.P. 78240 Mexico

[e] Now at Fraunhofer Inst. für Solar Energiesysteme, 79100 Freiburg, Germany

[f] Now at Technische Universitaät München, Garching, Germany

[g] Now at Fakultät für Physik, Univ. Freiburg, Germany

[h] Now at Departament of Physics and Astronomy, SUNY at Stony Brook, NY 11794-3800, USA

[i] Now at Max-Planck-Institut für Physik, München, Germany

[j] University of Iowa, Iowa City, IA 52242, USA

[k] Universitaät Mainz, Institut für Kernphysik, Germany

[l] Rutgers University,Piscataway, NJ 08854, USA

[m] *Permanent address:* CERN, 1211 Genève 23, Switzerland

[n] NIKEF, 1009 DB Amsterdam, The Netherlands

[o] Supported by the UK PPARC

[p] Supported by the Bundesministerium für Bildung, Wissenschaft, Forschung und Technologie, Germany, under contract numbers 05 5HD15I, 06 HD524I and 06 MZ5265

In the present paper we report on the inclusive production of $K^{\pm}_{890}$ mesons in nuclear targets by Σ^- and π^- of 345 GeV/c momentum and by neutrons of 260 GeV/c mean momentum.

The inclusive hadronic production of K_{890} in the central region at beam momenta of 6–400 GeV/c has been studied by several experiments using $\pi^{\pm}$, $K^{\pm}$ and proton beams [4]–[18]. At large x_F some experiments have studied only leading-particle channels, owing to a lack of statistics for other channels.

The results presented here are the first measurement of Σ^--induced K_{890} production cross sections. The results obtained simultaneously with π^- and n beams provide us with interesting complementary information, allowing to compare data from different beams measured in the same experiment. Together with the existing data on K_{890} production mentioned above and the large amount of data on hyperon and hyperon resonance production (see [32]–[34] and earlier references therein) there now exists a comprehensive set of data on inclusive hadronic production processes at large momenta, which allows stringent tests of existing models of hadron production.

We compare our experimental results with calculations using the Lund model (PYTHIA) [20]. and the quark-gluon string model (QGSM) [21]–[27] which was specially developed for soft hadroproduction phenomena at high energies.

2 Hyperon beam and experimental apparatus

The hyperon beam was derived from an external proton beam of the CERN-SPS, hitting a hyperon production target placed 16m upstream of the experimental target. Negative secondaries with a mean momentum of 345 GeV/c and a momentum spread $\sigma(p)/p \approx 9\%$ were selected in a magnetic channel. The production angles relative to the proton beam were smaller than 0.5 mrad. At the experimental target, the beam consisted of π^-, K^-, Σ^- and Ξ^- in the ratio 2.3: 0.025: 1: 0.012. A transition radiation detector (TRD) made up of 10 MWPCs interleaved with foam radiators allowed to suppress π^- at the trigger level. Typically, about $1.8 \cdot 10^5$ Σ^- and $4.5 \cdot 10^5$ π^- were delivered to the target during one SPS-spill, which had an effective length of about 1.5 s.

Σ^- decays upstream of the target were a source of neutrons used in our measurement as a neutron beam. The momenta of these neutrons were defined as the difference between the average Σ^- momentum and the momentum of the associated π^- measured in the spectrometer. The neutron spectrum had an average momentum of 260 GeV/c and a width of $\sigma(p)/p = 15\%$. More details can be found in [29].

The experimental target consisted of one copper and three carbon blocks arranged in a row along the beam, with thicknesses corresponding to 0.026 λ_I and three times 0.0083 λ_I, resp. At the target, the beam had a width of 3 cm and a height of 1.7 cm. Microstrip detectors upstream and downstream of the target allowed to measure the tracks of the incoming beam particle and of the charged particles produced in the target blocks. The target was positioned 14m upstream of the center of the Omega spectrometer magnet [30] so that a field-free decay region of 10m length was provided for hyperon and K^0_s decays. Tracks of charged particles were measured inside the magnet and in the field-free regions upstream and downstream by MWPCs and driftchambers, with a total of 130 planes. The Omega magnet provided a field integral of 7.5 Tm, and the momentum resolution achieved was $\sigma(p)/p^2 \approx 10^{-4}$ (GeV/c)$^{-1}$.

Downstream of the spectrometer, a ring-imaging Cherenkov detector, an electromagnetic calorimeter and a hadron calorimeter (SPACAL) were placed. In the present measurement we did not use these two detectors.

The main trigger selected about 25% of all interactions, using multiplicities measured in microstrip counters upstream and downstream of the target, and in scintillator hodoscopes and MWPCs behind the Omega magnet. Correlations between hits in different detectors were used in the trigger to increase the fraction of events with high-momentum particles, thus reducing background from low-momentum pions in the beam. In addition, a reduced sample of beam triggers was recorded for trigger calibration purposes. The results presented in this article are based on 100 million events recorded in 1993.

3 Event selection

The $K^{\pm}_{890}$ states were reconstructed from the $K^{\pm}_{890} \rightarrow K^0_s$ $\pi^{\pm}$, $K^0_s \rightarrow \pi^+\pi^-$ decay chain.

The interaction vertex had to contain at least two outgoing charged tracks reconstructed in the microstrip counters downstream of the target. At least one of them had to be connected to a track reconstructed in the spectrometer, so that it could be interpreted as a charged decay pion from a $K^{\pm}_{890}$ decay. The reconstructed vertex position had to be inside of a target block where in each coordinate an additional margin of 3σ was allowed.

For Σ^- and π^- interactions, the beam track reconstructed in the microstrip counters upstream of the target had to have a transverse distance to the interaction vertex of less than 6σ ($\sigma \approx 25\mu m$).

For neutron interactions, the beam track interpreted as the π^- track from a Σ^- decay had to have a transverse distance to the interaction vertex of more than 6σ. In addition, this assumed π^- track had to be connected to a track in the spectrometer corresponding to a negative particle with a momentum of less than 140 GeV/c, the maximal π^- momentum in $\Sigma^- \rightarrow n\pi^-$ decays at $< p > \approx$ 345 GeV/c. These cuts were optimized to separate Σ^-, π^- interactions from neutron interactions.

K^0_s candidates were selected from all pairs of positive and negative tracks which formed a vertex in the decay zone between the microstrip detectors downstream of the target and the Omega magnet. The distance between the two tracks at the decay point had to be smaller than 3 mm. The K^0_s trajectory reconstructed from the decay pions had to have a transverse distance to the interaction vertex of less than 12 mm. The effective $\pi^+\pi^-$ mass had

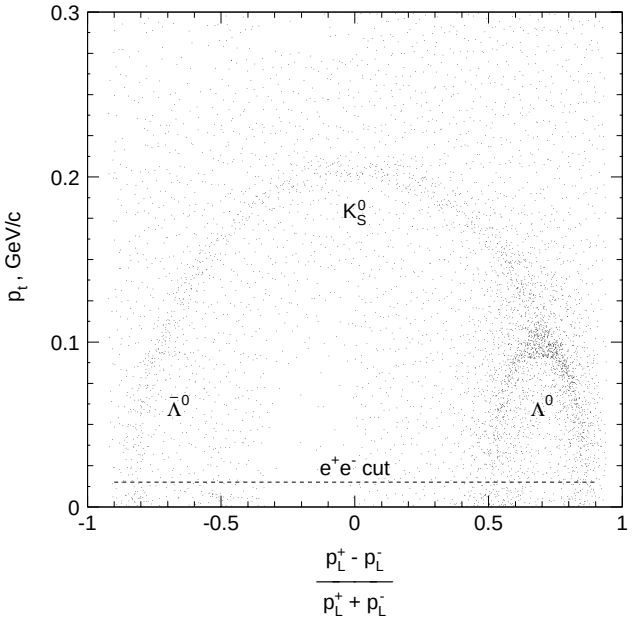

Fig. 1. Armenteros-Podolanski plot of the V^0. e^+e^- pairs were cut at $p_t = 0.015 GeV/c$. $p_L^{\pm}$ and p_t are the laboratory longitudial and transverse momenta of the decay tracks with the respect to the V^0 direction

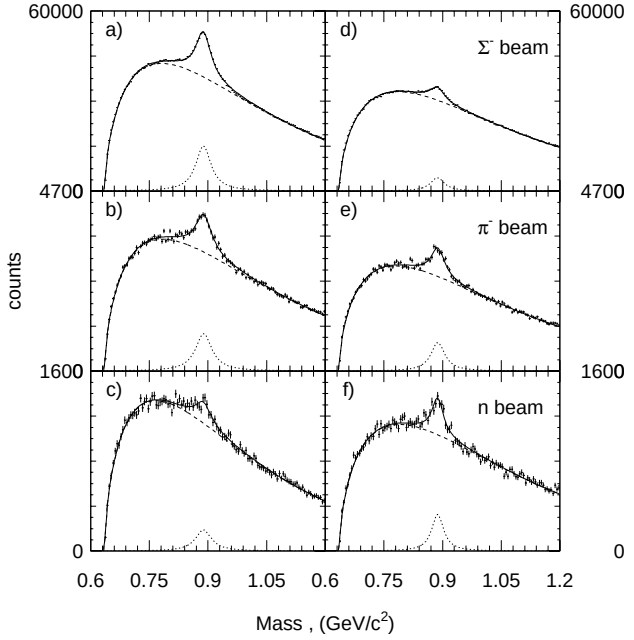

Fig. 2a–f. $K^0_S\pi^{\pm}$ effective mass distributions: $K^0_S\pi^-$ (a - c); $K^0_S\pi^+$ (d – f)

to be within 5 σ_E and 15 MeV/c^2 of the K^0_s mass, the mass error σ_E being typically 2.2 MeV/c^2. The K^0_s momentum had to be below 260 GeV/c. The K^0_s sample was contaminated by 4.5% of Λ^0 and 1.6% of $\overline{\Lambda}^0$as can be seen from Armenteros–Podolanski plot (Fig. 1) [31]. Ambiguous V^0 candidates were removed from the data and corresponding correction factors were applied in the cross section evaluation.

The contamination from e^+e^-pairs was suppressed by requiring that the transverse CMS momenta had to be greater than 15 MeV/c.

These K^0_s candidates were then combined with all charged particles coming from the primary vertex to form candidates for $K^{\pm}_{890} \rightarrow K^0_s\pi^{\pm}$ decays.

Figure 2 shows the observed $K^0_S\pi^{\pm}$ mass distributions. Clear signals are seen at the $K^{\pm}_{890}$ mass. The distributions were fitted with Voigt function (a convolution of a Breit-Wigner for the intrinsic width of the resonance and a gaussian for the mass resolution of the apparatus). The width of signals is dominated by the intrinsic width $\Gamma(K^{\pm}_{890}) = (47.9 \pm 1.2)$ MeV/c^2. The experimental mass resolution was estimated in Monte-Carlo simulations to be about 5 MeV/c^2 and was used in our fit. The shape of the background was determined by event mixing, combining the K^0_s candidates from a given event with the decay pion candidates from another event.

4 The $K^{\pm}_{890}$ production cross sections

The differential cross section as a function of the Feynman variable x_F and p_t^2 was calculated by the following formula:

$$\sigma(x_F, p_t^2) = \frac{N_{K(890)}(x_F, p_t^2)}{BR \cdot \varepsilon(x_F, p_t^2)\ N_b\ \rho\ l\ N_A/M}$$

Here $N_{K(890)}$ is the number of events in the K_{890} peak in particular (x_F, p_t^2) region, BR means branching ratio for the chain $K^{\pm}_{890} \rightarrow K^0_S\pi^{\pm}$, $K^0_S \rightarrow \pi^+\pi^-$, ε is the overall acceptance including reconstruction and trigger efficiencies, N_b is the number of incoming beam particles tagged as Σ^-, corrected for losses due to the deadtimes of the trigger and the data acquisition system. The $K^{\pm}_{890} \rightarrow K^0_S\pi^{\pm}$ decay branching ratio was set to be 2/3 as required by isospin conservation. M, ρ and l are the atomic mass, the density and the length of the target, N_A is the Avogadro number.

The hyperon beam actually contained different components as described in our previous publications [29,32]. The Σ^- sample identified by the TRD contained about (12±2)% of fast π^- , (2.0±0.5)% of K^- and (1.3±0.3)% of Ξ^- . The contamination from π^- interactions was corrected for using the cross sections observed in our experiment. For the contaminations from the small K^- and Ξ^- beam rates we assumed cross sections equal to the Σ^- cross sections, and added the amount of these contributions to the systematic errors. In the π^- sample identified by the TRD the total remaining contamination amounts to 1.%, mainly Σ^-. We corrected for the small contribution from Σ^- using our measured cross sections. The even smaller contributions from $\Xi^-$and K^- could safely be neglected.

The corrected differential production cross sections are shown in Figs. 3a–d and listed in Tables 3–7 for copper and carbon targets, respectively. Only fit errors are quoted here. To these fit errors we have to add systematic uncertainties of the reconstruction efficiency (≈ 15%) and the trigger efficiency (≈ 10%). The uncertainty from the Σ^-

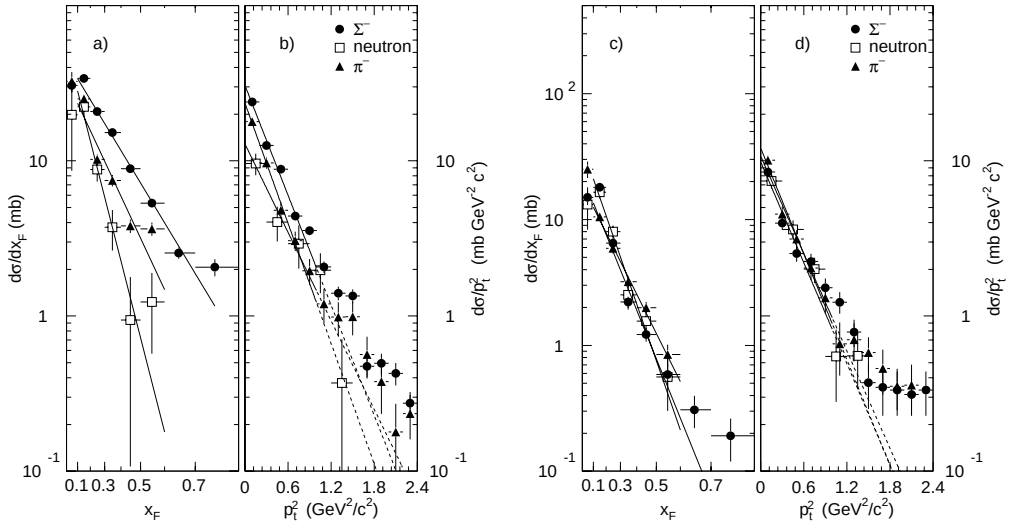

Fig. 3a–d. Differential cross sections of inclusive K^-_{890} production by Σ^-, neutrons and π^- in carbon

Table 1. Numbers of observed K^0_s decays and total inclusive $K^{\pm}_{890}$ production cross sections σ per nucleus for $x_F > 0$. σ_0 denotes the extrapolated cross sections per nucleon and α is the measured exponent in the A-dependence of the cross sections. An 18% systematic uncertainty has to be added to the statistical error of the cross section

particle	target	statistic	$\sigma, [mb]$	$\sigma_0, [mb]$	α
		Σ^- beam			
$K^-_{890}\to K^0_s\pi^-$	Cu	97896 ± 3060	$35. \pm 2.$		
	C	103825 ± 3185	12.0 ± 0.5		
	N			2.4 ± 0.3	0.64 ± 0.04
$K^+_{890}\to K^0_s\pi^+$	Cu	25337 ± 1233	11.7 ± 0.8		
	C	29116 ± 1434	4.4 ± 0.2		
	N			1.0 ± 0.2	0.59 ± 0.05
		π^- beam			
$K^-_{890}\to K^0_s\pi^-$	Cu	7362 ± 309	$25. \pm 2.$		
	C	6645 ± 280	8.4 ± 0.5		
	N			1.7 ± 0.3	0.65 ± 0.06
$K^+_{890}\to K^0_s\pi^+$	Cu	4288 ± 240	12.2 ± 0.9		
	C	4833 ± 245	4.8 ± 0.4		
	N			1.2 ± 0.3	0.56 ± 0.06
		neutron beam			
$K^-_{890}\to K^0_s\pi^-$	Cu	1227 ± 175	$13.2 \pm 2.$		
	C	1437 ± 172	5.7 ± 0.9		
	N			1.6 ± 0.7	0.5 ± 0.1
$K^+_{890}\to K^0_s\pi^+$	Cu	1609 ± 148	$15. \pm 2.$		
	C	1789 ± 143	4.2 ± 0.5		
	N			0.6 ± 0.2	0.7 ± 0.1

beam contaminations discussed above is 4% only. Adding the systematic errors quadratically results in a total systematic normalization error of 18%.

The differential cross sections were then parameterized by a function of the form:

$$\frac{d^2\sigma}{dp_t^2 dx_F} = C(1-x_F)^n \cdot exp(-Bp_t^2), \qquad (1)$$

which is based on quark counting rules and phase space arguments [36]. The three parameters C,n, and B were assumed to be independent of p_t^2 and x_F. The values of n and B obtained from the fits are listed in Table 2 for each target, and the fits are shown in the figures as straight lines over the fit range. No significant difference is observed between the values obtained from the copper and the carbon target.

Figure 4 show the nuclear mass dependence of $K^{\pm}_{890}$ production by Σ^- and π^- as a function of x_F (top) and p_t^2(bottom). The statistics of the neutron beam data were not sufficient for this analysis. The left-hand scales give

Table 2. The fit parameters n and B of the cross section parametrisation $d^2\sigma/dp_t^2 dx_F = C(1-x_F)^n exp(-Bp_t^2)$ (see text)

	Beam	Σ^-		π^-		Neutrons	
particle	target	n	B	n	B	n	B
$K^-_{890}\to K^0_s\pi^-$	Cu	3.0 ± 0.1	2.6 ± 0.1	3.6 ± 0.2	3.2 ± 0.2	4.5 ± 0.8	2.4 ± 0.7
	C	2.6 ± 0.1	2.7 ± 0.1	3.4 ± 0.2	3.0 ± 0.2	$6.0\pm1.$	2.2 ± 0.4
$K^+_{890}\to K^0_s\pi^+$	Cu	4.2 ± 0.4	2.2 ± 0.3	3.9 ± 0.3	2.2 ± 0.3	5.7 ± 0.5	1.9 ± 0.4
	C	4.8 ± 0.4	2.5 ± 0.3	3.9 ± 0.3	2.6 ± 0.3	5.7 ± 0.6	2.4 ± 0.5

Table 3. Differential production cross sections of K^-_{890} as a function of x_F in mb. An 18% systematic uncertainty has to be added to the statistical error of the cross section

Beam	Neutrons		π^-		Σ^-	
x_F	Copper	Carbon	Copper	Carbon	Copper	Carbon
0.0–0.1	$27.\pm17.$	$20.\pm11.$	$84.\pm13.$	$33.\pm5.$	$81.\pm9.$	$31.\pm3.$
0.1–0.2	$54.\pm10.$	$22.\pm3.$	$79.\pm5.$	$25.\pm2.$	$107.\pm4.$	$34.\pm1.$
0.2–0.3	$33.\pm6.$	$9.\pm1.$	$38.\pm3.$	10.2 ± 0.7	$63.\pm2.$	20.7 ± 0.7
0.3–0.4	$12.\pm4.$	$4.\pm1.$	$22.\pm2.$	7.5 ± 0.6	$47.\pm2.$	15.2 ± 0.5
0.4–0.5	$5.\pm2.$	0.9 ± 0.8	$12.\pm1.$	3.8 ± 0.4	$23.\pm1.$	8.9 ± 0.4
0.5–0.6	–	1.2 ± 0.7	–	3.6 ± 0.4	14.7 ± 0.8	5.3 ± 0.3
0.6–0.7	–	–	–	–	6.1 ± 0.6	2.6 ± 0.2
0.7–0.8	–	–	–	–	3.2 ± 0.6	2.1 ± 0.3

Table 4. Differential production cross sections of K^-_{890} as a function of p_t^2 in mb/(GeV/c)^2. An 18% systematic uncertainty has to be added to the statistical error of the cross section

Beam	π^-		Σ^-	
p_t^2	Copper	Carbon	Copper	Carbon
0.0–0.2	$61.\pm3.$	$18.\pm1.$	$68.\pm2.$	$24.\pm0.6$
0.2–0.4	$24.\pm2.$	9.7 ± 0.8	$34.\pm1.$	12.6 ± 0.5
0.4–0.6	$14.\pm2.$	4.8 ± 0.6	$19.\pm1.$	8.8 ± 0.4
0.6–0.8	$7.\pm1.$	3.1 ± 0.4	14.2 ± 0.8	4.4 ± 0.3
0.8–1.0	$7.\pm1.$	2.0 ± 0.4	11.1 ± 0.8	3.6 ± 0.2
1.0–1.2	2.7 ± 0.8	1.2 ± 0.3	7.1 ± 0.6	2.1 ± 0.2
1.2–1.4	3.4 ± 0.7	1.0 ± 0.2	6.4 ± 0.6	1.4 ± 0.1
1.4–1.6	1.3 ± 0.6	1.0 ± 0.2	4.1 ± 0.4	1.3 ± 0.1
1.6–1.8	1.8 ± 0.4	0.6 ± 0.2	3.4 ± 0.4	0.5 ± 0.1
1.8–2.0	1.3 ± 0.4	0.4 ± 0.1	2.5 ± 0.4	0.5 ± 0.1
2.0–2.2	1.9 ± 0.4	0.2 ± 0.1	1.5 ± 0.3	0.4 ± 0.1
2.2–2.4	0.7 ± 0.3	0.2 ± 0.1	1.3 ± 0.3	0.3 ± 0.1

the cross section ratio:

$$R = \frac{\sigma_{Cu}}{\sigma_C} \cdot \frac{A_C}{A_{Cu}} \tag{2}$$

The right-hand scales shows the corresponding values of α in the conventional parametrisation for the A dependence:

$$\sigma = \sigma_0 \cdot A^\alpha \tag{3}$$

The dashed lines correspond to α=2/3 and α=1, resp.

The observed values of α are close to 2/3. They show no clear dependence on either x_F or p_t^2. However, they are also compatible with the x_F–dependence observed in other experiments and which can be summarized as $\alpha(x_F) = 0.8 - 0.75x_F + 0.45x_F^2$ [37] (solid line in the upper part of each panel of Fig. 4).

The total production cross sections per nucleus for copper and carbon in the range $x_F > 0$ are listed in Table 1. Only statistical errors are shown.

The total production cross sections per nucleon for $x_F > 0$ were obtained by extrapolating the differential cross sections measured on Cu and C in each bin of x_F using the values of α obtained in the same bin. They are listed as σ_0 in Table 1.

5 Discussion

In this analysis two models have been considered as representing the theoretical grounds of the physics under study. These are the event generator PYTHIA [20] and so called quark-gluon string model (QGSM) [21]- [28].

In PYTHIA hadronic collisions are described in terms of the partonic subprocesses involving quarks and gluons (e.g. gluon-gluon fusion, quark-gluon scattering etc.). The corresponding cross sections are calculated according to standard QCD Feynman rules. We want to point out that PYTHIA was used with its default set of parameters, and no attempt was made to change them to obtain better fits to our experimental data, since this would destroy the

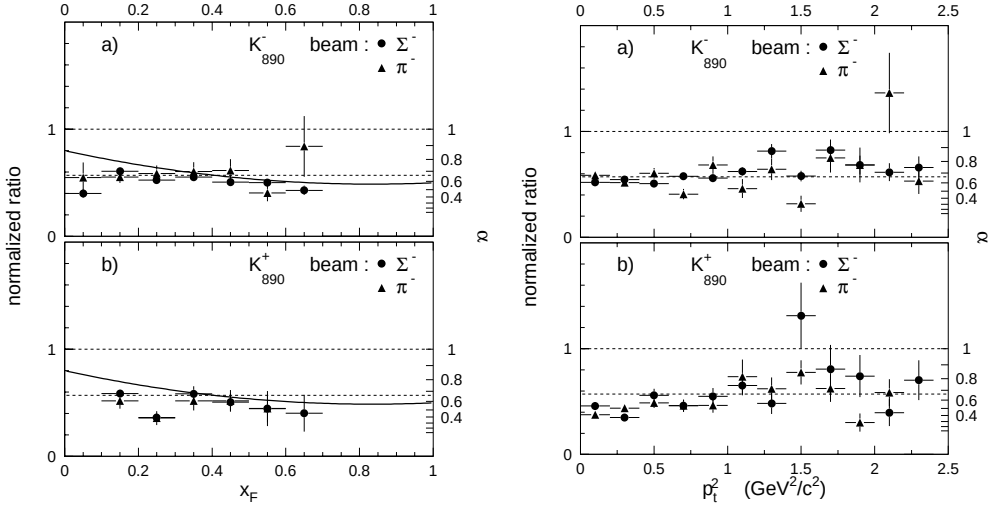

Fig. 4a,b. Normalized ratio R (see (2)) of K^-_{890} (upper panel) and K^+_{890} (lower panel) production by Σ^- and π^- in copper and carbon as a function of x_F (top) and p_t^2 (bottom). The right scale indicates the exponent α in the A^α dependence. The solid line in the upper part shows a polynomial fit to a compilation of target attenuation factors given in [37].

Table 5. Differential production cross sections of K^+_{890} as a function of x_F in mb. An 18% systematic uncertainty has to be added to the statistical error of the cross section

Beam	Neutrons		π^-		Σ^-	
x_F	Copper	Carbon	Copper	Carbon	Copper	Carbon
0.0–0.1	59.7 ± 20.9	13.2 ± 4.9	41.4 ± 8.2	25.1 ± 3.8	$48. \pm 7.$	$15. \pm 2.$
0.1–0.2	48.5 ± 6.4	16.5 ± 1.8	39.0 ± 3.0	10.5 ± 0.9	$45. \pm 2.$	18.0 ± 0.9
0.2–0.3	28.2 ± 3.7	8.0 ± 1.0	14.7 ± 1.6	5.9 ± 0.5	$12. \pm 1.$	6.5 ± 0.4
0.3–0.4	14.3 ± 1.9	2.5 ± 0.6	11.4 ± 1.0	3.2 ± 0.3	6.8 ± 0.7	2.2 ± 0.2
0.4–0.5	1.7 ± 1.1	1.6 ± 0.4	6.9 ± 0.7	2.0 ± 0.2	3.2 ± 0.4	1.2 ± 0.1
0.5–0.6	1.5 ± 0.7	0.6 ± 0.3	–	0.8 ± 0.2	1.3 ± 0.3	0.6 ± 0.1
0.6–0.7	–	–	–	–	0.7 ± 0.3	0.3 ± 0.1
0.7–0.8	–	–	–	–	0.5 ± 0.2	0.2 ± 0.1

agreement with other experimental results (for a discussion of this point, see [34]).

On the contrary QGSM is based on an essentially nonperturbative approach. The production of particles is treated as a Reggeon exchange process, where parameters of the exchanged Reggeon are determined by the quark content of the initial and final state hadrons.

Coming now to the experimental results summarized in Fig. 5, one can tell that the agreement with theoretical estimations is certainly better for K^{*+} mesons than for K^{*-}, and in the case of pion or neutron beam it may be classified as quantitative for both models.

In Σ^- beam PYTHIA reproduces the x_F spectrum shape of K^{*+} much better than QGSM. PYTHIA prediction is in a good agriment with K^{*-} data in case of neutron beam as well. In two other beams PYTHIA predicts too strong leading effect. Contrarily QGSM systematically underestimates the production of K^{*-} mesons in baryon beams. Surprisingly, the model does not show significant difference in the production of K^{*-} mesons by Σ^- and by pions, although the experimental data show a clear leading particle effect produced by the strange quark of the Σ^- beam particle.

We have observed in a separate simulation that even the sole contribution of the strange quark fragmentation into kaon shows a too steep x_F dependence. Therefore, the reason for the disagreement may be seen in the fact that the model attributes too small momentum to the strange quark in the hyperon. As a consequence, this slow s-quark cannot produce a large-x_F kaon.

On the other hand, we have complementary evidence that QGSM attributes a too large momentum to diquarks in baryon. This may be deduced from our earlier data on the production of Ξ^- hyperons by Σ^-, π^- and neutron beams. As we have already pointed out in the previous publication [34], the QGSM overestimates the leading effect in the Σ^- and neutron beams predicting too flat x_F spectra for Ξ^- hyperons. Also, the predictions made for Σ^- and neutron beams appear to be too close to each other, as if there would be no essential difference between the fragmentation of strange ds and non-strange dd diquarks.

The p_t^2 distributions are very similar for all targets and beams particles. They follow a Gaussian behavior up to 1.–1.2 GeV/c and then show a nongaussian behavior as was already observed in our previous studies of hyperon production [32,34].

Table 6. Differential production cross sections of K^+_{890} as a function of p_t^2 in mb/(GeV/c)^2. An 18% systematic uncertainty has to be added to the statistical error of the cross section

Beam	π^-		Σ^-	
p_t^2	Copper	Carbon	Copper	Carbon
0.0–0.2	21.5 ± 1.8	10.1 ± 0.7	19.8 ± 1.0	8.5 ± 0.4
0.2–0.4	11.8 ± 1.5	4.5 ± 0.5	7.8 ± 0.7	4.0 ± 0.3
0.4–0.6	8.9 ± 1.2	3.1 ± 0.4	7.7 ± 0.7	2.5 ± 0.2
0.6–0.8	5.1 ± 0.9	2.0 ± 0.3	5.2 ± 0.5	2.2 ± 0.2
0.8–1.0	3.3 ± 0.7	1.3 ± 0.3	4.6 ± 0.5	1.5 ± 0.2
1.0–1.2	2.7 ± 0.7	0.7 ± 0.2	4.0 ± 0.4	1.2 ± 0.1
1.2–1.4	2.4 ± 0.5	0.7 ± 0.2	2.2 ± 0.4	0.8 ± 0.1
1.4–1.6	2.6 ± 0.4	0.6 ± 0.1	2.7 ± 0.3	0.4 ± 0.1
1.6–1.8	1.5 ± 0.4	0.5 ± 0.1	1.3 ± 0.2	0.3 ± 0.1
1.8–2.0	0.7 ± 0.3	0.4 ± 0.1	1.1 ± 0.2	0.3 ± 0.1
2.0–2.2	0.9 ± 0.2	0.4 ± 0.1	0.8 ± 0.2	0.3 ± 0.1
2.2–2.4	–	–	1.1 ± 0.2	0.3 ± 0.1

Table 7. Differential cross sections of K^-_{890} and K^+_{890} production by neutrons as a function of p_t^2 in mb/(GeV/c)^2. An 18% systematic uncertainty has to be added to the statistical error of the cross section

	K^-_{890}		K^+_{890}	
p_t^2	Copper	Carbon	Copper	Carbon
0.0–0.3	$25. \pm 4.$	$10. \pm 2.$	$25. \pm 3.$	7.4 ± 0.8
0.3–0.6	$12. \pm 3.$	4.0 ± 1.0	$11. \pm 2.$	3.6 ± 0.5
0.6–0.9	$3. \pm 2.$	2.9 ± 0.9	$9. \pm 2.$	2.0 ± 0.4
0.9–1.2	$2. \pm 2.$	2.0 ± 0.6	$5. \pm 1.$	0.5 ± 0.3
1.2–1.5	$3. \pm 1.$	0.4 ± 0.3	$2. \pm 1.$	0.6 ± 0.2

The dependence of the $K^{*\pm}$ production cross section on the atomic number shows the same behavior as observed for other hadrons.

Further data on V^0 production cross sections and on correlations in V^0V^0 pair production from experiment WA89 are presently under analysis [38]. The results may lead to a clearer understanding of the shortcomings of both models.

6 Conclusions

We have presented the first measurement of $K^{\pm}_{890}$ production by Σ^- hyperons at 345 GeV/c in fixed carbon and copper targets. This measurement was supplemented by measurements of $K^{\pm}_{890}$ production by neutrons and pions, exactly in the same experimental conditions.

The data clearly show the well known leading particle effect. The x_F–dependence of the observed production cross sections has been compared to calculations using the Lund model (PYTHIA) and the quark-gluon string model. Both models fail to describe the x_F dependence of the cross sections in particular for K^-_{890} production by Σ^-, where the data show a clear leading particle effect.

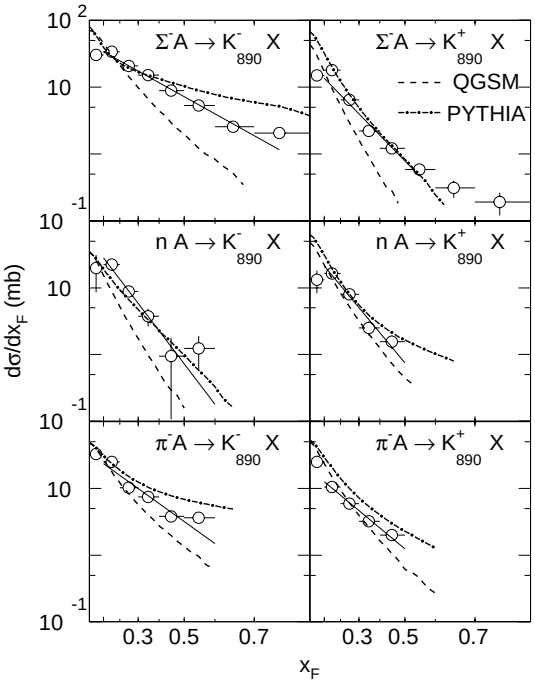

Fig. 5. Comparison of the measured differential cross sections with PYTHIA and QGSM predictions. The solid line shows the fit of experimental data by (1)

Acknowledgements. It is a pleasure to thank J. Zimmer and G. Konorova for their support in setting up and running the experiment. We are also indebted to the staff of the CERN Omega spectrometer group for their help and support, to the CERN EBS group for their work on the hyperon beam line and to the CERN accelerator group for their continuous efforts to provide good and stable beam conditions. We thank B.Kopeliovich for helpful discussions.

References

1. F. Takagi, Phys. Rev. D **27**, 1461 (1983)
2. T. Tashiro et al., Z. Phys. C **35**, 21 (1987); T. Tashiro, H. Noda, K. Kinoshita, Z. Phys. C **39**, 499 (1988)
3. R.A.M.S. Nazareth, N. Prado, T. Kodama, Phys. Rev. D **40**, 2861 (1989;)R.A.M.S. Nazareth, T. Kodama, D.A. Portes, Phys. Rev. D **46**, 2896 (1992)
4. C.Evangelista et al., Phys. Lett. **70B**, 373 (1977)
5. R.Singer et al., Nucl. Phys. **B135**, 265 (1978)
6. C.Cochet et al., Nucl. Phys. **B155**, 333 (1979)
7. H.Kichimi et al., Phys. Rev. **D20**, 37 (1979); Lett. N. Cim. **24**, 129 (1979)
8. R.Sugahara et al., Nucl. Phys. **B156**, 237 (1979)
9. K.Böckmann et al., Nucl. Phys. **B166**, 284 (1980)
10. I.V.Ajinenko et al., Z. Physik **C5**, 177 (1980)
11. D.Brick et al., Phys. Rev. **D25**, 2248 (1982)
12. P.V.Chliapnikov et al., Z. Physik **C12**, 105 (1982)
13. R.Göttgens et al., Z. Physik **C12**, 323 (1982)
14. M.Barth et al., Nucl. Phys. **B223**, 296 (1983)
15. E.A.Starchenko et al., Z. Physik **C16**, 181 (1983)
16. R.Bailey et al., Z. Physik **C24**, 111 (1984)
17. A.Napier et al., Phys. Lett. **149B**, 514 (1984)

18. S.Mikocki et al., Phys. Rev. **D34**, 42 (1986)
19. The Particle Data Group, Eur. J. Phys, **C3**, 1 (1998)
20. T. Sjöstrand, Computer Phys. Comm. **82**, 74 (1994)
21. A. Capella et al., Z. Phys. C **3**, 329 (1970)
22. K.A. Ter-Martirosyan, Phys. Lett. B **44**, 377 (1973)
23. M. Ciafaloni, G. Marchesini, G. Veneziano, Nucl. Phys. B **98**, 472 (1975)
24. A.B. Kaidalov, Sov. JETP Lett. **32**, 494 (1980)
25. A.B. Kaidalov, K.A. Ter-Martirosyan, Sov. J. Nucl. Phys. **39**, 1545 (1984)
26. A.I. Veselov, O.I. Piskunova, K.A. Ter-Martirosyan, Phys. Lett. B **158**, 175 (1985)
27. A.B. Kaidalov, O.I. Piskunova, Sov. J. Nucl. Phys. **41**, 1278 (1985;)A.B. Kaidalov, O.I. Piskunova, Z. Phys. C **30**, 145 (1986;)A.B. Kaidalov, Sov. J. Nucl. Phys. **45**, 1450 (1987)
28. S.P. Baranov, Lebedev Institute of Physics report **42** (1998)
29. Yu.A.Alexandrov et al., CERN-SL-97-60 EA and Nucl. Instr. Meth. **A408**, 359 (1998)
30. W. Beusch, CERN/SPSC/77-70
31. J.Podolansky, R.Armenteros, Phyl. Mag. **45**, 13 (1954)
32. Yu.A.Alexandrov et al., Z. Phys. **C76**, 35 (1997)
33. Yu.A.Alexandrov et al., Eur.Phys.J. **C5**, 621 (1998)
34. Yu.A.Alexandrov et al., Eur.Phys.J. **C11**, 271 (1999)
35. D. Drijard et al., Nucl. Instr. Meth. **225**, 367 (1984); D. L'Hote, Nucl. Instr. Meth. **A337**, 544 (1994)
36. R. Blankenbecler, S.J. Brodsky, Phys. Rev. **D10**, 2973 (1974)
37. W.M. Geist, Nucl. Phys. A**525**, 149c (1991)
38. Strange particle production with Σ^-, π^- and neutrons in Hyperon experiment WA89 at CERN. Fourth International Conference on Hyperons, Charm and Beauty Hadrons. By WA89, Nuclear Physics **93** (Proc. Suppl.) (2001) 62